DALTON
FULL PAPER

Synthesis and characterisation of $[Ru_6C(CO)_{14}]$ cluster complexes of some [2.2]- and [2.2.2]-cyclophane ligands

Paul Schooler, Brian F. G. Johnson,* Laura Scaccianoce and Rosemary Tregonning

University Chemical Laboratory, Lensfield Road, Cambridge, UK CB2 1EW

Received 19th April 1999, Accepted 10th June 1999

Some $[Ru_6C(CO)_{14}]$ cluster complexes bearing the [2.2]ortho-, *anti*-[2.2]meta- and [2.2.2]para-cyclophane ligands have been prepared, isolated and characterised. The molecular structure of two new compounds $[Ru_6C(CO)_{14}$-(meta-$C_{16}H_{16}$)] **2** and $[Ru_6C(CO)_{14}$(para-$C_{24}H_{24}$)] **4** have been established by X-ray diffraction studies which show that the cyclophane ligands are bound in an apical η^6 mode in both cases. This is at variance with the face-capping μ_3-η^2:η^2:η^2 mode observed in the previously reported structure of $[Ru_6C(CO)_{14}$(para-$C_{16}H_{16}$)] **1**. Spectroscopic evidence obtained for $[Ru_6C(CO)_{14}$(ortho-$C_{16}H_{16}$)] **3** suggests that the cyclophane ligand is bound in an apical η^6 mode too. The synthesis of **1** *via* the redox coupling of $[Ru_5C(CO)_{14}]^{2-}$ with $[Ru(\eta^6$-$C_{16}H_{16})(NCMe)_3]^{2+}$ is presented as an alternative to the thermolysis of $[Ru_3(CO)_{12}]$ with [2.2]paracyclophane in heptane.

Introduction

The transition metal carbonyl cluster chemistry of the cyclophane ligands has so far been mainly limited to [2.2]paracyclophane and its mono-ring substituted derivatives.[1,2] Examples are known which encompass a range of metal nuclearities from two[3] to eight[4] and a variety of arene bonding modes including η^6, μ-η^3:η^3 and μ_3-η^2:η^2:η^2.[3–5] Among these compounds there is a marked tendency of the [2.2]paracyclophane ligand to adopt the facial μ_3 co-ordination mode. The most prevalent example of this behaviour is in the hexaruthenium carbido cluster $[Ru_6C(CO)_{14}$(arene)] where the simpler arenes (benzene, toluene, xylene and mesitylene) tend to adopt the apical η^6 mode.[6] This effect has been rationalised both in terms of the electronic properties and the molecular structure of the ligand.[2] Owing to the extensive overlap of the π molecular orbitals between the two aromatic decks, the [2.2]paracyclophane ligand has a superior donor capability over simpler arenes and as such can provide a sufficient supply of electron density to donate to three metal atoms and not just one.[7] An alternative explanation involves the inherent distortion of the aromatic rings in the [2.2]paracyclophane ligand.[8] These are convex, bulging outward from the centre of the molecule as a consequence of strong interarene repulsions. This results in the outward orientation of the π molecular orbitals in such a way that they would be expected to interact more effectively with a trimetallic face rather than a single metal apex. In order to extend previous work and to provide evidence that validates such explanations we initiated a study into how a change in the bridge substitution pattern of a [2.2]cyclophane (and therefore the degree of the overlap of the π molecular orbitals and their orientation in space) affects cluster co-ordination behaviour, concentrating upon the interaction of the hexanuclear carbido cluster unit $[Ru_6C(CO)_{14}]$ with the *anti*-[2.2]metacyclophane,[9] [2.2]orthocyclophane[10] and [2.2.2]paracyclophane ligands.[11] It has been found that all of these ligands adopt an apical η^6 mode which is at variance with the behaviour of [2.2]paracyclophane as illustrated in Fig. 1.[6]

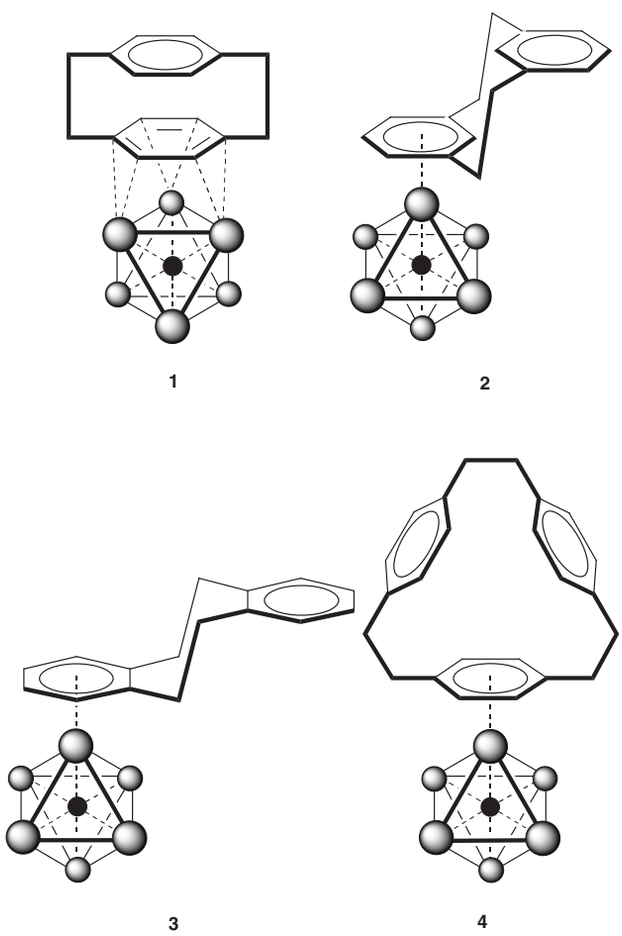

Fig. 1 The compounds $[Ru_6C(CO)_{14}(\mu_3$-η^2:η^2:η^2-para-$C_{16}H_{16})]$ **1**, $[Ru_6C(CO)_{14}(\eta^6$-meta-$C_{16}H_{16})]$ **2**, $[Ru_6C(CO)_{14}(\eta^6$-ortho-$C_{16}H_{16})]$ **3** and $[Ru_6C(CO)_{14}(\eta^6$-para-$C_{24}H_{24})]$ **4**.

Results and discussion

The thermolysis of *anti*-[2.2]metacyclophane with three molar equivalents of $[Ru_3(CO)_{12}]$ in octane under reflux over a 6 h period affords $[Ru_6C(CO)_{14}(\eta^6$-meta-$C_{16}H_{16})]$ **2** as the major product. Similarly, analogous reactions involving [2.2]orthocyclophane and [2.2.2]paracyclophane over an 8 h period yield $[Ru_6C(CO)_{14}(\eta^6$-ortho-$C_{16}H_{16})]$ **3** and $[Ru_6C(CO)_{14}(\eta^6$-para-$C_{24}H_{24})]$ **4** as the major products, respectively. In any case, compounds **2**, **3** and **4** may be separated from the starting materials and binary metal carbonyl by-products by

chromatography on silica using dichloromethane–hexane (1 : 2 v/v) as eluent.

The initial mass and infrared spectroscopic evidence suggested that compounds **2**, **3** and **4** possess structures that were related to that of the benzene cluster $[Ru_6C(CO)_{14}(\eta^6\text{-}C_6H_6)]$ (see Table 1):[6] the parent ion peak for compounds **2** and **3** was observed at *m*/*z* 1219 by FAB mass spectrometry while for **4** it was at *m*/*z* 1324. This is consistent with the formulation $[Ru_6C(CO)_{14}(\text{cyclophane})]$ in all three cases. The infrared spectra of compounds **2**, **3** and **4** were found to be similar in appearance to each other and to that of the benzene cluster $[Ru_6C(CO)_{14}(\eta^6\text{-}C_6H_6)]$.[6] The absence of a distinctive strong carbonyl stretching band at approximately 2035 cm^{-1} (as for $[Ru_6C(CO)_{14}(\mu_3\text{-}\eta^2\text{:}\eta^2\text{:}\eta^2\text{-para-}C_{16}H_{16})]$) excluded the facial co-ordination of the cyclophane ligands in **2**, **3** and **4**.[6] Hence, the *anti*-[2.2]meta-,[9] [2.2]ortho-[10] and [2.2.2]para-cyclophane[11] ligands in these compounds were assigned apical η^6 bonding modes at variance with the $\mu_3\text{-}\eta^2\text{:}\eta^2\text{:}\eta^2$ mode observed for the [2.2]paracyclophane ligand in compound **1**.[6]

This assignment was confirmed for compounds **2** and **4** by an X-ray diffraction study. For **2**, a crystal obtained from a concentrated dichloromethane–toluene solution at −20 °C was used for structural analysis. The molecular structure of compound **2** is shown in Fig. 2 with an alternative top view in Fig. 3. Relevant bond distances and angles are shown in Table 2 while crystal data and measurement details are given in the Experimental section. The molecular structure of compound **2** is based upon a hexaruthenium octahedral framework which surrounds a central carbide atom. The metal–metal bond distances range from 2.846(2) to 2.970(2) Å while the metal–carbide distances range from 1.914(13) to 2.105(13) Å. It can clearly be seen that the encapsulated interstitial carbide atom is displaced considerably towards the Ru(1), the metal atom

Table 1 Spectroscopic data for compounds **1**–**4**

Complex	*m*/*z* [a]	$\tilde{\nu}_{CO}/cm^{-1}$ [b]	δ [c]
1	1219 (calc. 1218)	2076m, 2035s, 2023vs, 1980m, 1938m, 1835w(br)	7.44 (s, 4 H), 3.43 (s, 4 H), 3.38 (m, 4 H), 2.99 (m, 4 H)
2	1219 (calc. 1218)	2077m, 2023vs, 1814w (br)	7.41 (t, 1 H, *J* 7.5), 7.14 (d, 2 H, *J* 7.5), 5.53 (t, 1 H, *J* 6.1), 5.37 (d, 2 H, *J* 6.1), 4.34 (s, 1 H), 3.09 (s, 1 H), 3.35–3.27 (m, 2 H), 2.91–2.82 (m, 2 H), 2.40–2.32 (m, 2 H), 1.68–1.61 (m, 2 H)
3	1219 (calc. 1218)	2075m, 2023vs, 1814w (br)	7.02–6.97 (m, 2 H), 6.92–6.88 (m, 2 H), 5.32–5.23 (m, 2 H), 5.16–5.11 (m, 2 H), 3.39–3.28 (m, 2 H), 3.18–3.05 (m, 2 H), 2.89–2.78 (m, 2 H), 2.65–2.53 (m, 2 H)
4	1324 (calc. 1323)	2074m, 2023vs, 1814w (br)	6.79 (d, 4 H, *J* 8.1), 6.69 (d, 4 H, *J* 8.1), 5.46 (s, 4 H), 2.89 (s, 4 H), 2.86 (pt, 4 H, *J* 6.7), 2.50 (pt, 4 H, *J* 6.7)

[a] FAB-MS, 3-nitrobenzyl alcohol matrix. [b] In CH_2Cl_2. [c] In $CDCl_3$, *J* in Hz.

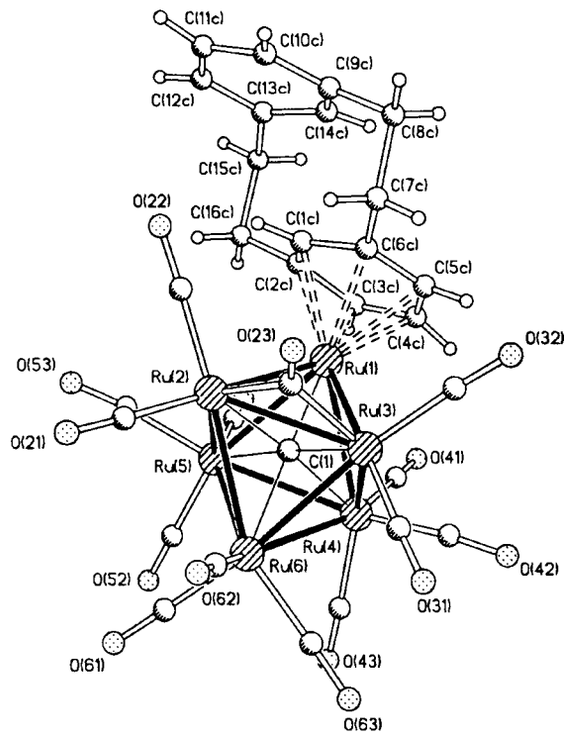

Fig. 2 The molecular structure of $[Ru_6C(CO)_{14}(\text{meta-}C_{16}H_{16})]$ **2**.

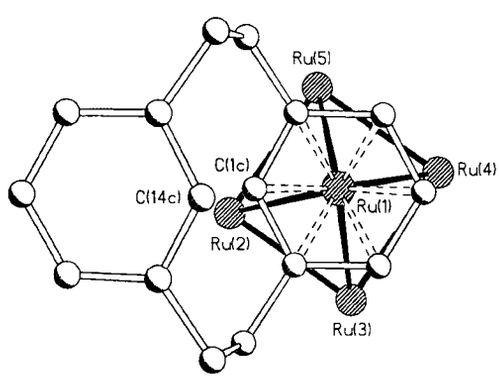

Fig. 3 An alternative top view of the molecular structure of $[Ru_6C(CO)_{14}(\text{meta-}C_{16}H_{16})]$ **2** (carbonyl ligands and cyclophane protons omitted for clarity).

Table 2 Important bond lengths (Å) for $[Ru_6C(CO)_{14}(\text{meta-}C_{16}H_{16})]$ **2**

Ru(1)–Ru(2)	2.889(2)	C(1)–Ru(1)	1.914(13)	Ru(1)–C(1c)	2.213(13)
Ru(1)–Ru(3)	2.857(2)	C(1)–Ru(2)	2.077(13)	Ru(1)–C(2c)	2.344(14)
Ru(1)–Ru(4)	2.882(2)	C(1)–Ru(3)	2.054(13)	Ru(1)–C(3c)	2.280(13)
Ru(1)–Ru(5)	2.873(2)	C(1)–Ru(4)	2.062(13)	Ru(1)–C(4c)	2.222(13)
Ru(2)–Ru(3)	2.877(2)	C(1)–Ru(5)	2.065(13)	Ru(1)–C(5c)	2.267(12)
Ru(2)–Ru(5)	2.966(2)	C(1)–Ru(6)	2.105(13)	Ru(1)–C(6c)	2.265(13)
Ru(2)–Ru(6)	2.881(2)				
Ru(3)–Ru(4)	2.970(2)	C(1c)–C(2c)	1.42(2)	C(15c)–C(16c)	1.58(2)
Ru(3)–Ru(6)	2.846(2)	C(1c)–C(6c)	1.41(2)	C(9c)–C(10c)	1.40(2)
Ru(4)–Ru(5)	2.853(2)	C(2c)–C(3c)	1.45(2)	C(9c)–C(14c)	1.40(2)
Ru(5)–Ru(6)	2.929(2)	C(3c)–C(4c)	1.41(2)	C(10c)–C(11c)	1.38(2)
		C(4c)–C(5c)	1.41(2)	C(11c)–C(12c)	1.40(2)
		C(5c)–C(6c)	1.41(2)	C(12c)–C(13c)	1.40(2)
		C(7c)–C(8c)	1.57(2)	C(13c)–C(14c)	1.41(2)

Table 3 Important plane angles in [2.2]metacyclophane and $[Ru_6C(CO)_{14}(meta\text{-}C_{16}H_{16})]$ **2** with reference to Fig. 4

Angle/°	"Free" ligand	Compound **2**
α	3.1	4.8
β	9.5	9.2
γ	9.5	8.2
δ	3.1	3.7

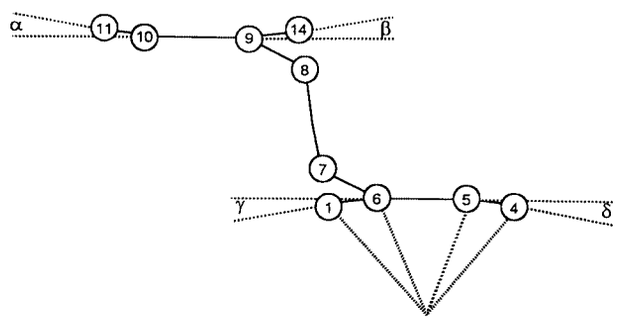

Fig. 4 Labelling of plane angles in [2.2]metacyclophane and $[Ru_6C(CO)_{14}(meta\text{-}C_{16}H_{16})]$ **2**.

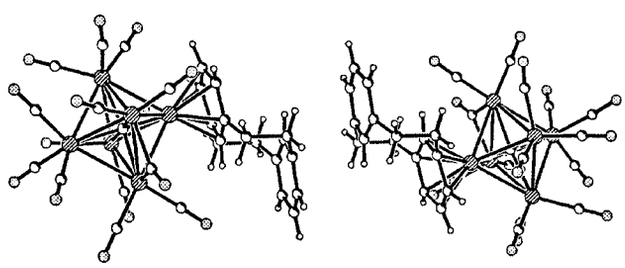

Fig. 5 The graphite type packing motif observed in the crystal structure of $[Ru_6C(CO)_{14}(meta\text{-}C_{16}H_{16})]$ **2**.

involved in the η^6 co-ordination of an *anti*-[2.2]metacyclophane ligand: the shortest metal–carbide distance involves Ru(1) while the longest involves Ru(6), the metal atom in the position *trans* to Ru(1). Such carbide drift is common in arene carbido clusters and is thought to occur because the arene is a poorer π acceptor than the carbonyl ligands it formally replaces.[12] The remainder of the cluster co-ordination sphere is occupied by fourteen carbonyl ligands which are all terminally bonded with the exception of CO(23) which bridges the Ru(2)–Ru(3) edge. The mean plane of the bound ring of the aforementioned cyclophane ligand is tilted by 5.3° with respect to the underlying {Ru(2)Ru(3)Ru(4)Ru(5)} square toward this edge. This is presumably as a result of steric repulsion, and is rotated such that the Ru(1)–C(1c) and Ru(1)–R(2) bonds are almost eclipsed in the top view (Fig. 3). The metal–ligand carbon bond lengths can be divided into two sets. The bow and stern carbon atoms of the bound aromatic ring C(1c) and C(4c) are closest to the metal apex, Ru(1), at 2.213(13) and 2.222(13) Å, respectively. The others vary somewhat particularly Ru(1)–C(2c), at 2.344(14) Å, is some 0.06 Å longer than the others indicating that the ligand is not symmetrically co-ordinated.

The reduction in the transannular π electron repulsions in compound **2** compared to those in the "free" ligand is apparent from the degree of deformation of the aromatic rings (see Fig. 4 and Table 3). The intraannular bow carbon atoms of the co-ordinated ring C(1c) and of the unco-ordinated ring C(14c) are displaced out of the aromatic plane at an angle of 8.2 (γ) and 9.2° (β), respectively, compared to a value of 9.5° in the "free" ligand.[9] Hence, the distance between these intraannular carbon atoms falls from 2.689(1) to 2.54(2) Å upon co-ordination, indicating the reduction in π electron density within the cyclophane. A search of the Cambridge Crystallographic Database indicates that this may be the shortest intraannular carbon–carbon distance within a [2.2]metacyclophane molecule determined so far (*cf.* the next shortest distance of 2.601(12) Å in meta-$C_{16}H_{16}$·TCNE).[13] The opposite effect is observed for the other extraannular stern carbon atoms, C(4c) of the co-ordinated ring and C(11c) of the unco-ordinated ring, which are pushed further out of the aromatic plane at an angle of 3.7 (δ) and 4.8° (α), respectively, compared to the "free" ligand at 3.1°.[9]

The crystalline structure was found to be comprised of two cyclophane clusters and two disordered dichloromethane molecules per unit cell. The disorder observed located one of the solvent chlorine atoms unequally over three sites. It is of note that an interesting graphitic packing motif is observed within the crystal structure of compound **2** (see Fig. 5). This involves the pairing of molecules such that the bound ring of one cyclophane molecule is directly over the free ring of that in its partner and *vice versa*. The interannular carbons C(14) on partnered molecules were found to be separated by only 3.288 Å.

The ^{1}H NMR of compound **2** was as anticipated for η^6 bound *anti*-[2.2]metacyclophane ligand. It contains a triplet at δ 7.41 and a doublet at 7.14 (1:2 integral ratio with coupling constant J 7.5 Hz) corresponding to the extraannular protons of the free aromatic ring {H(11), and H(10) and H(12), respectively}, while a triplet at δ 5.53 and a doublet at 5.37 (1:2 integral ratio with coupling constant J 6.1 Hz) corresponding to the extraannular protons of the bound ring {H(4), and H(3) and H(5), respectively}. The intraannular protons H(1c) of the bound ring and H(14c) of the free ring are observed as singlets at δ 3.09 and 4.34, respectively, the former shifted to lower frequency by some −1.16 ppm and the latter to higher frequency by +0.09 ppm.[14] It is noteworthy that the H(1c) and H(14c) proton signals are observed at particularly high field even though the cyclophane is bound in an η^6 mode. This effect originates from the structure of the ligand in which protons H(1c) and H(14c) are located over the face of the opposing aromatic ring and thus experience an electronic shielding effect.[14] The bridging protons are observed as four multiplets of equal integral at δ 3.35–3.27, 2.91–2.82, 2.40–2.32 and 1.68–1.61.

For compound **4** a crystal obtained by the slow evaporation of a concentrated dichloromethane–pentane solution at 20 °C was used for structural analysis. As anticipated the molecular structure is closely related to that of compound **2**. It is illustrated in Fig. 6 with the relevant bond distances shown in Table 4, while crystal data and measurement details are given in the Experimental section. The cluster framework again is based upon a *closo* octahedron which encapsulates a central carbido atom. The metal–metal bond lengths range from 2.836(3) to 2.987(3) Å while the metal–carbide distances range from 1.94(2) to 2.09(2) Å with the shortest contact to Ru(1) and the longest to Ru(6). One of the aromatic rings of the cyclophane ligand is co-ordinated in an η^6 mode upon Ru(1) with metal–carbon distances ranging between 2.10(3) and 2.38(3) Å. It should be noted, however, that the cyclophane ligand is severely disordered over two sites with almost equal occupancies and the co-ordinated aromatic rings in the two positions have complementary long and short metal–carbon contacts (see Fig. 7). The remainder of the cluster co-ordination sphere is occupied by fourteen carbonyl ligands of which one is edge bridging, namely CO(23).

The ^{1}H NMR of compound **4** was as expected for an η^6 bound [2.2.2]paracyclophane ligand. A singlet at δ 5.46 clearly corresponds to the ring protons of the bound aromatic ring. This is observed at much higher field than those of the "free" ligand due to both a reduction in ring current and to direct metal anisotropy (*cf.* δ 6.23).[11] The protons of the free aromatic rings were observed as doublets at lower field than for the "free"

Table 4 Important bond lengths (Å) for $[Ru_6C(CO)_{14}(para\text{-}C_{24}H_{24})]$ **4**

Ru(1)–Ru(2)	2.878(3)	Ru(1)–C(1)	1.94(2)	Ru(1)–C(1c)	2.36(3)
Ru(1)–Ru(3)	2.876(3)	Ru(2)–C(1)	2.07(2)	Ru(1)–C(2c)	2.38(3)
Ru(1)–Ru(4)	2.884(3)	Ru(3)–C(1)	2.05(2)	Ru(1)–C(3c)	2.26(3)
Ru(1)–Ru(5)	2.865(3)	Ru(4)–C(1)	2.05(2)	Ru(1)–C(4c)	2.12(2)
Ru(2)–Ru(3)	2.864(3)	Ru(5)–C(1)	2.06(2)	Ru(1)–C(5c)	2.10(2)
Ru(2)–Ru(5)	2.917(3)	Ru(6)–C(1)	2.09(2)	Ru(1)–C(6c)	2.16(2)
Ru(2)–Ru(6)	2.878(3)				
Ru(3)–Ru(4)	2.987(3)			Ru(1)–C(1′)	2.19(3)
Ru(3)–Ru(6)	2.836(3)			Ru(1)–C(2′)	2.15(3)
Ru(4)–Ru(5)	2.857(3)			Ru(1)–C(3′)	2.20(4)
Ru(4)–Ru(6)	2.875(3)			Ru(1)–C(4′)	2.28(3)
Ru(5)–Ru(6)	2.927(3)			Ru(1)–C(5′)	2.32(3)
				Ru(1)–C(6′)	2.27(2)

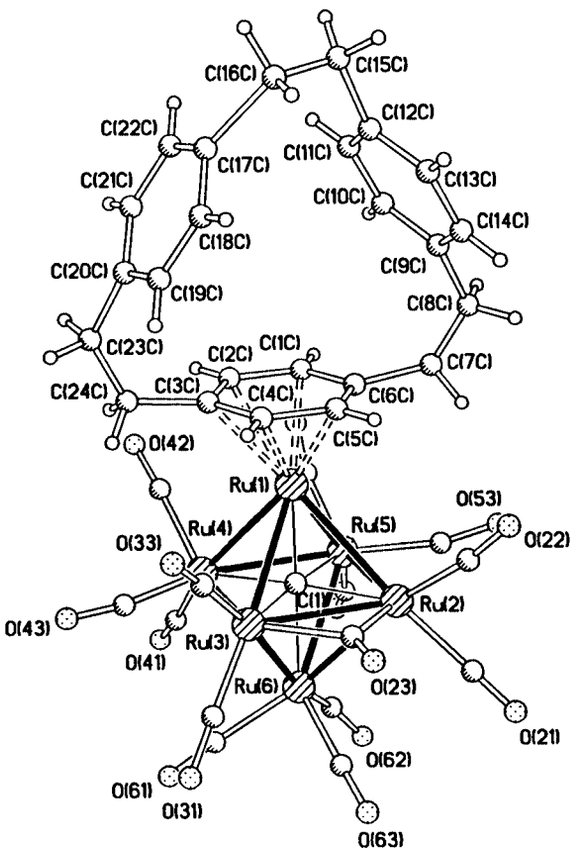

Fig. 6 The molecular structure of $[Ru_6C(CO)_{14}(para\text{-}C_{24}H_{24})]$ **4**.

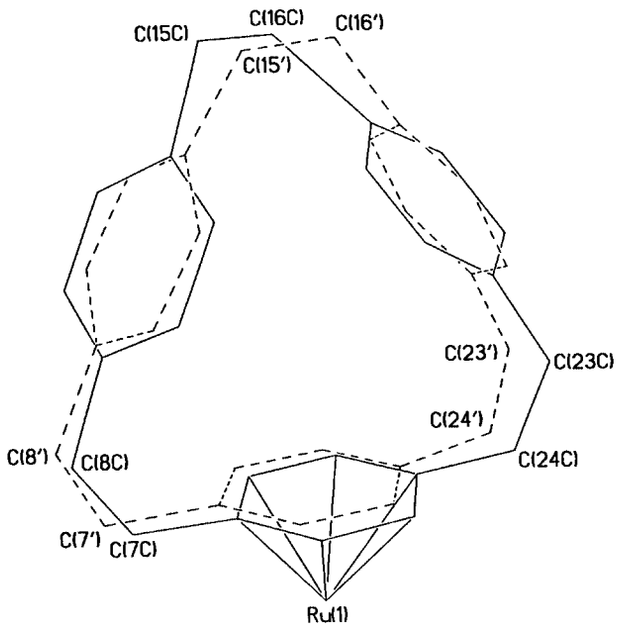

Fig. 7 The disorder of the cyclophane ligand observed in the crystalline structure of $[Ru_6C(CO)_{14}(para\text{-}C_{24}H_{24})]$ **4**.

ligand (δ 6.79 and 6.69 with a coupling constant of J 8.1 Hz)[11] presumably due to the reduction in shielding provided by the bound ring owing to loss of ring current. The ethano bridge protons were also shifted downfield by 0.03–0.42 ppm. A singlet δ 2.89 and two pseudo-triplets at δ 2.86 and 2.50 (J 6.7 Hz) all of equal intensity were also observed, the foremost signal corresponding to the ethano bridge protons that are located directly over the bound aromatic ring {those attached to C(15c)–C(16c)}.

Unfortunately crystals of compound **3** suitable for X-ray diffraction analysis have not yet been obtained. Thus the compound was characterised only by ^{1}H NMR in addition to the initial mass and infrared spectroscopic studies. With two multiplets observed in the appropriate shift range {δ 5.32–5.23 and 5.16–5.11 for the co-ordinated aromatic protons}, the ^{1}H NMR spectrum supports the assignment of an η^6 bonding mode for the [2.2]orthocyclophane ligand. The free aromatic protons are also observed as two multiplets but at lower field at δ 7.02–6.97 and 6.92–6.88 while the bridging protons are observed as four multiplets at δ 3.39–3.28, 3.18–3.05, 2.89–2.78 and 2.65–2.53.

Apical or facial?

In summary, [2.2]paracyclophane is found to adopt a facial μ_3 bonding mode upon co-ordination to the hexaruthenium carbido core, while the [2.2]meta and [2.2]ortho isomers along with the [2.2.2]paracyclophane ligand prefer to adopt the apical η^6 bonding mode, only interacting with a single metal atom. There are two possible explanations for this behaviour.

First, the superior donor capability of [2.2]paracyclophane over *anti*-[2.2]meta- and [2.2]ortho- and [2.2.2]para-cyclophane ligands may be responsible, whereby the extensive overlap of π molecular orbitals in the para isomer can provide a sufficient supply of electron density to donate to three metal atoms.[7] There is little, if any, overlap of π molecular orbitals in the meta and ortho isomers and hence they can be envisaged as only being able to support a single metal atom, while the overlap in the [2.2.2]para ligand is drastically reduced compared to that in [2.2]paracyclophane.[9–11] This effect has been demonstrated electrochemically for the $[Ru_6C(CO)_{14}(C_{16}H_{16})]$ isomers, whereby the para isomer was far more difficult to reduce than either the meta or ortho (compare −0.937, −0.893 and −0.891 V, respectively, for an irreversible reduction, see Table 5).

The cyclic voltammogram of $[Ru_6C(CO)_{14}(meta\text{-}C_{16}H_{16})]$ **2**, for example, is illustrated in Fig. 8, which clearly shows the irreversible reduction potential (wave A) of the compound and the oxidation potential of its daughter product (wave B). Waves C and D correspond to the reversible oxidation of ferrocene which was used as an internal standard.

Table 5 The irreversible reduction potentials of compounds **1**, **2** and **3** and the oxidation potentials of their daughter products

Compound	Substitution	Potential/V	
		For irreversible reduction of the product	For oxidation of the daughter product
1	Para	−0.937	+0.086
2	Meta	−0.893	−0.145
3	Ortho	−0.891	−0.555

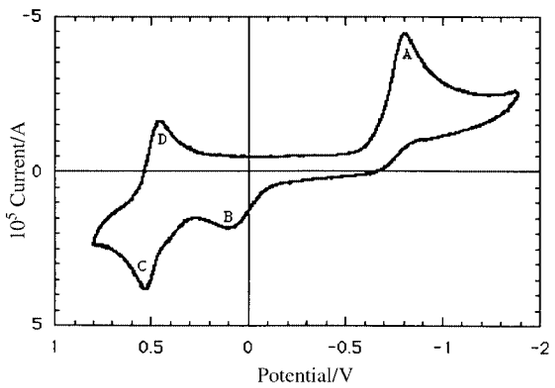

Fig. 8 The cyclic voltammogram showing the irreversible reduction potential (wave A) of $[Ru_6C(CO)_{14}(meta\text{-}C_{16}H_{16})]$ **2** and the oxidation potential of its daughter product (wave B). Waves C and D correspond to the reversible oxidation of ferrocene.

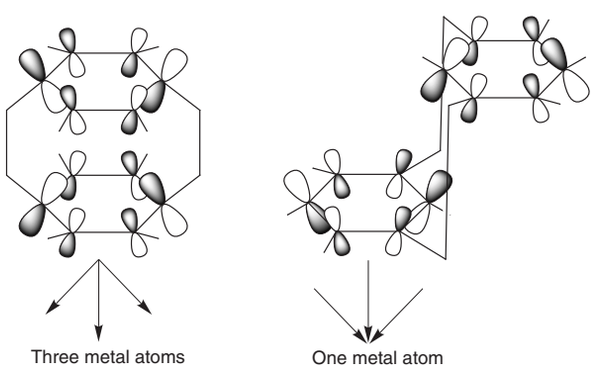

Fig. 9 The π orbitals in [2.2]paracyclophane and *anti*-[2.2]metacyclophane oriented such that the former is predisposed to interact with a metal face while the latter is predisposed to interact with a single metal atom.

Alternatively, the difference in co-ordination mode may be explained by the inherent distortion of the aromatic rings within the cyclophane ligands themselves (see Fig. 9). Since the aromatic rings are convex in [2.2]paracyclophane,[8] bulging outwards from the centre of the molecule due to interarene repulsions, the π orbitals are oriented in such a way that they would be expected to interact more effectively with a trimetallic face than a single metal atom. However, in the meta isomer the aromatic rings are concave, with the π orbitals oriented towards a focal point and thus the ligand is predisposed to interact with only a single metal atom.[9] Furthermore, the distortion of the rings in both [2.2]para- and [2.2]meta-cyclophanes cause the aromatic C–H bonds to bend out of the plane. In [2.2]paracyclophane this occurs such that the C–H bonds point toward the centre of the molecule and in [2.2]metacyclophane such that they point away. Since the C–H bonds bend away from the underlying metal triangle in, for example $[Os_3(CO)_9(\mu_3\text{-}C_6H_6)]$,[15] it is therefore unsurprising that [2.2]paracyclophane adopts the facial bonding mode on the hexaruthenium cluster. Similarly, since the C–H bonds point toward the metal atom in mononuclear arene complexes it is again not surprising that the [2.2]metacyclophane ligand adopts an apical bonding mode. In [2.2]orthocyclophane and [2.2.2]paracyclophane the aromatic rings are near planar and therefore presumably the preference of these ligands for the apical η^6 mode is not as strong as that of the meta isomer.[10,11]

The preference of the [2.2]paracyclophane ligand for the facial $\mu_3\text{-}\eta^2:\eta^2:\eta^2$ bonding mode has also been shown by the redox coupling of $[Ru(C_{16}H_{16})(NCMe)_3)]^{2+}$ with cluster anions (see Scheme 1). It has been known for sometime that the combination of the anionic cluster $[Ru_5C(CO)_{14}]^{2-}$ with the cationic benzene capping fragment $[Ru(\eta^6\text{-}C_6H_6)(NCMe)_3]^{2+}$ results in the formation of the arene cluster $[Ru_6C(CO)_{14}(\eta^6\text{-}C_6H_6)]$, in which the arene ligand is bound in an η^6 apical bonding mode (see Scheme 1).[12] However, we have found that the analogous combination of the anionic cluster $[Ru_5C(CO)_{14}]^{2-}$ with the cationic cyclophane capping fragment $[Ru(\eta^6\text{-}C_{16}H_{16})(NCMe)_3]^{2+}$ results in the formation of the known cluster $[Ru_6C(CO)_{14}(\mu_3\text{-}\eta^2:\eta^2:\eta^2\text{-}C_{16}H_{16})]$ **1**,[6] in which the arene ligand is facially co-ordinated despite the [2.2]paracyclophane ligand being bound in an η^6 mode in the precursor complex.[16] Thus it would appear reasonable to assume that cluster **1** is formed *via* rapid rearrangement of the less stable $[Ru_6C(CO)_{14}(\eta^6\text{-}C_{16}H_{16})]$ **1′** encounter complex. The mechanism by which this process occurs is presumably ring slippage whereby the cyclophane migrates from an apical to a facial bonding mode, possibly *via* a μ edge-bridging mode. Hence the redox coupling of $[Ru_5C(CO)_{14}]^{2-}$ with $[Ru(\eta^6\text{-}C_{16}H_{16})(NCMe)_3]^{2+}$ is both presented as an alternative to the thermolysis of $[Ru_3(CO)_{12}]$ with [2.2]paracyclophane in heptane and also as an illustration of the [2.2]paracyclophane ligand's preference of the facial bonding mode upon the hexaruthenium carbido core.[6]

Conclusion

It has been found that the [2.2]ortho-, *anti*-[2.2]meta- and [2.2.2]para-cyclophane ligands interact with the $[Ru_6C(CO)_{14}]$ cluster unit *via* an apical η^6 arene bonding mode. This is at variance with the behaviour of the [2.2]paracyclophane ligand which interacts *via* a facial $\mu_3\text{-}\eta^2:\eta^2:\eta^2$ mode. These observations can be rationalised to some extent by consideration of the molecular or electronic structure of these ligands.

Experimental

Synthesis and characterisation

All syntheses were performed with the exclusion of air using solvents dried by conventional procedures. The compound $[Ru_3(CO)_{12}]$ and the cyclophane ligands were prepared by literature procedures without modification. Other chemicals were purchased from Sigma-Aldrich Ltd. Infrared spectra were recorded in dichloromethane using NaCl cells (0.5 mm path length) on a Perkin-Elmer 1600 Series FTIR spectrometer, FAB mass spectra on a Kratos MS890 spectrometer in the positive mode using a 3-nitrobenzyl alcohol matrix and ^1H NMR spectra on a Bruker DPX-250 FT instrument, run using 5 mm 528-PP quartz tubes. Cyclic voltammograms were recorded on an Autolab PSTAT 10 device interfaced to a Dell 466DL computer using the General Purpose Electrochemical GPES4 Windows software package. A standard three electrode cell was used which was equipped with a working micro, platinum counter and Ag–AgCl reference electrode. Tetra-*n*-butylammonium tetrafluoroborate (8.2 g, 25 mmol) was used as the inert electrolyte dissolved in distilled dichloromethane (50 ml). Voltammetric measurements were carried out under a nitrogen atmosphere at a scan rate of 0.1 V s^{-1}. Intensity data from single crystals was measured on a Rigaku AFC-7R for

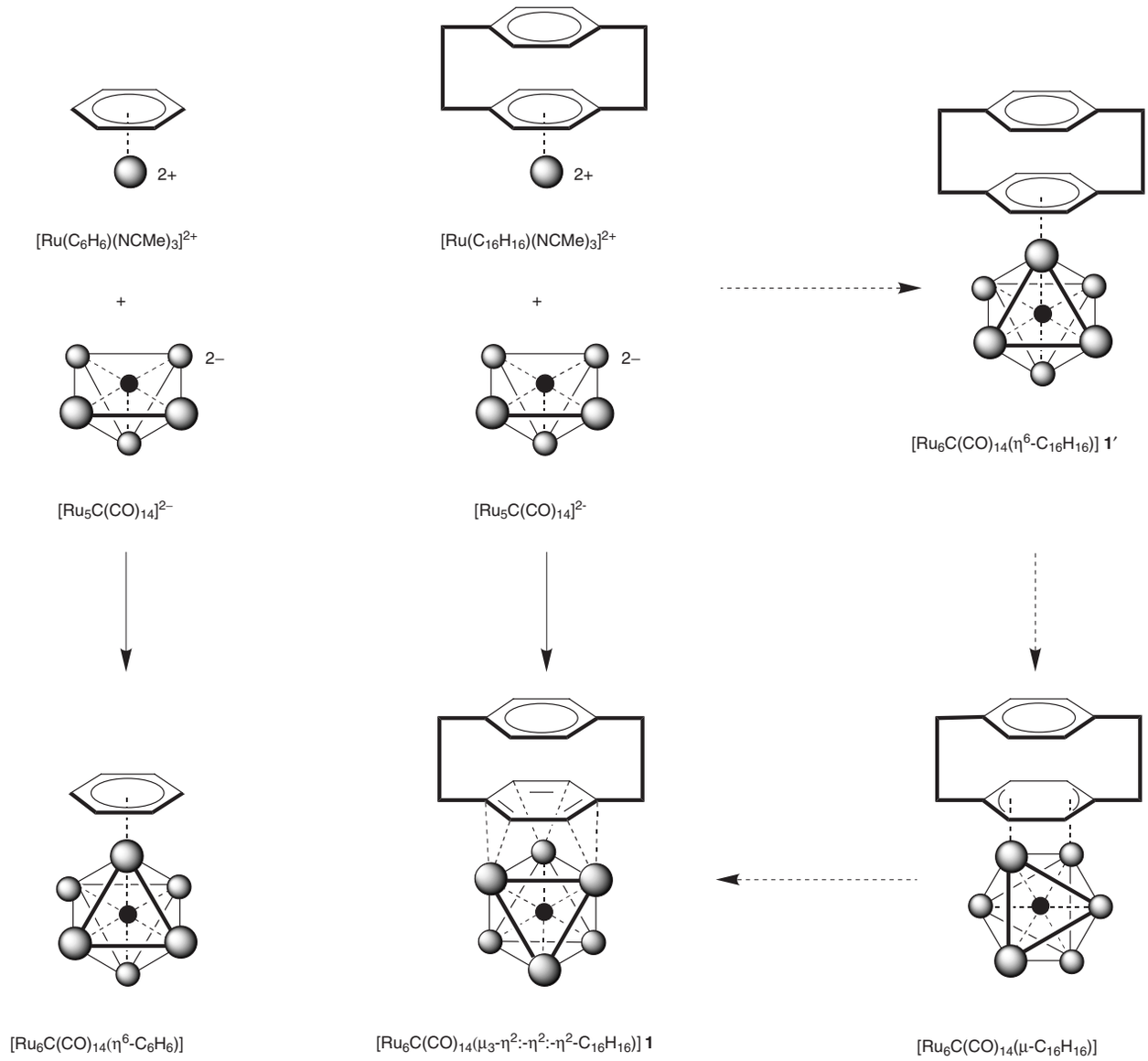

Scheme 1 The formation of $[Ru_6C(CO)_{14}(\eta^6\text{-}C_6H_6)]$ and $[Ru_6C(CO)_{14}(\mu_3\text{-}\eta^2\!:\eta^2\!:\eta^2\text{-}C_{16}H_{16})]$ **1** *via* redox coupling. The formation of compound **1** possibly occurs *via* unstable η^6 and μ modes.

complex **2** and a Nicolet R3v/m diffractometer for **4**, in the ω–θ mode.

Syntheses

$[Ru_6C(CO)_{14}(\mu_3\text{-para-}C_{16}H_{16})]$ 1. The compound $[\{Ru(C_{16}H_{16})Cl_2\}_2]$ (22 mg, 28 μmol) and $AgBF_4$ (12 mg, 56 μmol) were dissolved in acetone (10 ml). After 1 h the silver chloride precipitated was removed by filtration through Celite revealing a clear yellow solution. The solvent was replaced with dichloromethane and the new solution added dropwise over 5 min to $[N(PPh_3)_2]_2[Ru_5(CO)_{14}]$ (80 mg, 56 μmol) dissolved in dichloromethane (10 ml). The solvent was then removed under vacuum and the residue obtained separated into its component compounds by column chromatography using dichloromethane–hexane (1:2, v/v) as the eluent. The $[Ru_6C(CO)_{14}(\mu_3\text{-}\eta^2\!:\eta^2\!:\eta^2\text{-}C_{16}H_{16})]$ **1** (red-orange, yield 50 mg, 42 mmol, 53%) was then purified by thin layer chromatography using the same solvent ratio before characterisation.

$[Ru_6C(CO)_{14}(\eta^6\text{-meta-}C_{16}H_{16})]$ 2. A suspension of $[Ru_3(CO)_{12}]$ (960 mg, 1.5 mmol) in octane (20 ml) containing [2.2]metacyclophane (104 mg, 500 μmol) was heated to reflux. Heating was discontinued after 6 h and the solvent removed under vacuum. The residue was separated into its component compounds by column chromatography using dichloromethane–hexane (1:2, v/v) as eluent. The $[Ru_6C(CO)_{14}(\eta^6\text{-meta-}C_{16}H_{16})]$ **2** (red, yield 49 mg, 40 μmol, 8%) was then purified by TLC eluting with the same solvent ratio before characterisation. The synthesis of compounds **1**, **3** and **4** can be effected in an analogous fashion (red, yields 18, 6 and 30%, respectively).

Crystal structure determinations

Crystal data for $[Ru_6C(CO)_{14}(\eta^6\text{-meta-}C_{16}H_{16})]$ 2. $C_{32}H_{18}Cl_2O_{14}Ru_6$ **2**·CH_2Cl_2, $M = 1303.78$, triclinic, space group $P\bar{1}$, $a = 11.433(2)$, $b = 17.780(2)$, $c = 9.467(1)$ Å, $\alpha = 95.94(1)$, $\beta = 97.71(1)$, $\gamma = 102.34(1)°$, $U = 1845.5(4)$ Å^3, $T = 293(2)$ K, $Z = 2$, $D_c = 2.346$ g cm^{-3}, $F(000) = 1240$, red block, μ(Mo-Kα) = 2.604 mm^{-1}.

Structure solution and refinement. The structure was solved by direct methods (SHELX 86)[17] and refined against F^2 using all data (SHELX 93).[17] Only the Ru and O atoms were modelled with anisotropic displacement parameters. A difference map showed peaks consistent with a full weight CH_2Cl_2 molecule. One of the chlorine atoms in this solvent molecule was, however, disordered in and about a local mirror plane. At

convergence the conventional R factor was 5.02% [based on F and 3262 data with $F > 2\sigma(F)$] and $wR2$ was 19.79% (based on F^2 and all 4775 unique data used in refinement) for 322 parameters. The final difference map extrema were +1.404 and −1.588 e Å^{-3}.

Crystal data for [$Ru_6C(CO)_{14}(\eta^6$-para-$C_{24}H_{24})$] 4. $C_{39}H_{24}O_{14}Ru_6$, $M = 1323.05$, monoclinic, space group $C2/c$, $a = 29.386(13)$, $b = 15.601(6)$, $c = 18.629(8)$ Å, $\beta = 103.82(3)°$, $U = 8293(5)$ Å^3, $T = 291$ K, $Z = 8$, $D_c = 2.12$ g cm^{-3}, $F(000) = 5072$, μ(Mo-Kα) = 2.154 mm^{-1}.

Structure solution and refinement. The structure was solved by direct methods and refined against F^2 using all data (SHELX 97).[17] All non-H atoms except those of one disordered cyclophane ligand were modelled with anisotropic displacement parameters. A difference map showed that the cyclophane ligand was disordered over two conformations with equal occupancies. At convergence the conventional R factor was 9.51% [based on F and 3134 data with $F > 2\sigma(F)$] and $wR2$ was 30.9% (based on F^2 and all 5144 unique data used in refinement) for 395 parameters. The final difference map extrema were +1.617 and −2.185 e Å^{-3}.

CCDC reference number 186/1510.

See http://www.rsc.org/suppdata/dt/1999/2743/ for crystallographic files in .cif format.

Acknowledgements

We would like to thank the EPSRC, the University of Cambridge and the Newton Trust (P. S.) for financial support, Professor Henning Hopf of the Technische Universität Braunschweig, Germany for his involvement in this project and also Dr John E. Davies for collecting X-ray diffraction data on our behalf.

References

1 C. J. Brown and A. C. Farthing, *Nature* (*London*), 1949, **164**, 915.
2 B. F. G. Johnson, C. M. Martin and P. Schooler, *Chem. Commun.*, 1998, 1239.
3 A. J. Blake, P. J. Dyson, B. F. G. Johnson and C. M. Martin, *J. Chem. Soc.*, *Chem. Commun.*, 1994, 1471.
4 See, for example, C. M. Martin, A. J. Blake, P. J. Dyson, S. L. Ingham and B. F. G. Johnson, *J. Chem. Soc.*, *Chem. Commun.*, 1995, 555.
5 D. Braga, F. Grepioni, P. J. Dyson, B. F. G. Johnson and C. M. Martin, *J. Chem. Soc.*, *Dalton Trans.*, 1995, 909.
6 D. Braga, F. Grepioni, E. Parisini, P. J. Dyson, A. J. Blake and B. F. G. Johnson, *J. Chem. Soc.*, *Dalton Trans.*, 1993, 2951.
7 P. J. Dyson, D. G. Humphrey, J. E. McGrady, D. M. P. Mingos and D. J. Wilson, *J. Chem. Soc.*, *Dalton Trans.*, 1995, 4039.
8 H. Hope. J. Bernstein and K. N. Trueblood, *Acta Crystallogr.*, *Sect. B*, 1972, **28**, 1733.
9 Y. Kai, *Acta Crystallogr.*, 1977, **33**, 754.
10 P. Domiano, P. Cozzini, R. M. Claramunt, J. L. Lavandera, D. Sanz and J. Elguero, *J. Chem. Soc.*, *Perkin Trans. 2*, 1992, 1609.
11 J. L. Piere, P. Baret, P. Chautemps and A. Armand, *J. Am. Chem. Soc.*, 1981, **103**, 2986.
12 D. Braga, P. J. Dyson, F. Grepioni and B. F. G. Johnson, *Chem. Rev.*, 1994, **94**, 909.
13 C. Cohen-Addad, A. Renault, G. Commandeur and P. Baret, *Acta Crystallogr.*, *Sect. C*, 1988, **44**, 914.
14 R. Paioni and W. Jenny, *Helv. Chim. Acta*, 1969, **52**, 2041.
15 M. P. Gomez-Sal, B. F. G. Johnson, J. Lewis, P. R. Raithby and A. H. Wright, *J. Chem. Soc.*, *Chem. Commun.*, 1985, 1682.
16 R. T. Swann, A. W. Hanson and V. Boekelheide, *J. Am. Chem. Soc.*, 1986, **108**, 3324.
17 G. M. Sheldrick, SHELX 86, *Acta Crystallogr.*, *Sect. A*, 1990, 467; SHELX 93, University of Göttingen, 1993; SHELX 97, University of Göttingen, 1997.

Paper 9/03103K